Final Report for:

"Estimating Unmetered Groundwater Irrigation Demand with High-Resolution Remote Sensing Data"

Project ID 1545

Reclamation Science and Technology Program
Funding Year 2012

Principal Investigator: Eve Halper, PhD.

Project Summary:

This project intended to answer the questions:

1. Can irrigated residential landscapes be effectively separated from vegetation supported by natural water sources using high-resolution pattern analysis techniques and LIDAR derived hydrography?

2. Does the combination of multispectral imagery and LIDAR data provide enough information to categorize high and low water demanding plant species?

3. Can a reasonable estimate of evapotranspiration (ET) of this vegetation be generated using a combination of a remote-sensing derived vegetation index, commonly available meteorological data and plant-specific ET coefficients?

4. How do these estimates compare with the values currently being used for domestic well irrigation demand?

Unfortunately, the National Agricultural Imagery Program (NAIP) 1 meter data did not have a high enough resolution to allow for the development of a reliable method to distinguish irrigated from naturally supported vegetation. The residential area of interest had very few lawns, so textural metrics were not effective. In addition, our study area contained regions of high elevation that received large amounts of rainfall, so a threshold NDVI method was not viable, either. Some progress was made in distinguishing rooftops by color, with the assumption that high-NDVI pixels near rooftops were likely to be irrigated. White roofs were easily distinguished, but newer homes with "earth-tone" roofs proved very difficult to isolate. Future work, if any, will require the use of an object recognition program, such as eCognition, to distinguish and categorize image objects by shape, color and other attributes.

LIDAR data provided by Fort Huachuca also proved to be of insufficient resolution to distinguish types of vegetation on the landscape. The bare earth and first return data were both 1.5 m resolution, which was down-sampled to 1 m for comparison with the NAIP data. Alignment between the two data sets was not perfect, and led to difficulties in interpretation. Another issue was the different times of acquisition: the LIDAR was collected in late September (post-monsoon), while the NAIP imagery was acquired in pre-monsoon, early June. The vegetation conditions in the two data sets were quite different and made it impractical to integrate them. The LIDAR derived hydrography was not effective in distinguishing irrigated and non-irrigated vegetation.

We intended to isolate irrigated vegetation within the high resolution image and use the MODIS evapotranspiration product (250 m pixel) to estimate water use over time. However, the vegetated patches in our images were extremely small compared to the size of MODIS pixels. We tried to establish a relationship between the mean NDVI of the MODIS pixel "footprint" in our study area and the MODIS NDVI product. However, the vegetated area within the study area was so small, no effect could be seen in the NDVI values of the 250 m MODIS pixels.

In conclusion, it may be possible to answer the above questions with better resolution data sets, or similar data sets in a different study area, with larger vegetation patches, more distinct irrigated vegetation, or where irrigated plant types are very different from background vegetation. However, in this southeastern Arizona landscape, such an analysis was not possible.

More information on specific aspects of the research are provided in the following attachment, provide by the other investigators.

Attachment 1:
"Estimating Unmetered Groundwater Irrigation Demand with High-Resolution Remote Sensing Data: Description of Methodologies and Products", by Wim van Leeuwen and Kyle Hartfield, Arizona Remote Sensing Center, The University of Arizona.

Attachment 2:
Integration of High-Resolution Imagery with Meteorological Data to Estimate Evapotranspiration, by Pamela Nagler, Ed Glenn and Eve Halper

Estimating Unmetered Ground Water Irrigation Demand with High-Resolution Remote Sensing Data

Description of Methodologies and Products

Wim van Leeuwen* and Kyle Hartfield*

in collaboration with Eve Halper, Stuart Marsh, Steve Yool, and Pamela Nagler

***Arizona Remote Sensing Center**

1955 E. Sixth Street, Suite 205
The University of Arizona
Tucson, AZ 85721
Phone: 520 626-0058 Fax: 520 621-3816
e-mail: leeuw@ag.arizona.edu ; kylehartfield@gmail.com

August 2012

CONTENTS

NAIP TO LANDSAT REFLECTANCE CALIBRATION

The Sierra Vista Sub Watershed (SVSW) was used to determine the correct National Agriculture Imagery Program (NAIP) tiles to employ for the study. It was determined that 89 tiles, with 1 meter nominal spatial resolution, encompassed the study area with some tiles extending outside of the boundaries of the SVSW. The tiles were mosaicked using the Mosaic Wizard tool within ERDAS Imagine 9.3.

A Landsat scene captured May 27, 2010 for Path35 Row 38 was downloaded from the USGS Global Visualization Viewer in order to calibrate the NAIP data. The Landsat data were run through the LEDAPS surface reflectance correction model to remove the influences of atmosphere on the image data values. The LEDAPS model also converted the data from Digital Numbers (DNs) to reflectance values.

15 points were selected within the study area, 5 representing vegetation, 5 representing dark objects, and 5 representing bright objects, on both the NAIP and Landsat data. The 15 points were used to create a scatterplot comparing the values in the blue, green, red, and near-infrared bands of the NAIP and Landsat data. A polynomial regression line was used to determine the correlation between the NAIP and Landsat values. All four bands exhibited an R^2 above 0.89 so it was determined the polynomial equations would be used to calibrate the NAIP data to the Landsat data (Figure 1).

Model Maker in ERDAS Imagine 9.3 was used to process each of the four NAIP bands through the corresponding polynomial equation. Once the model was completed each of the bands was checked to verify the conversion of the raw digital to reflectance values. A false color image was created based on the multispectral NAIP reflectance data (Figure 2).

CREATION OF EVAPOTRANSPIRATION RASTER USING NDVI

The four bands were then stacked together and Model Maker was used to create a Normalized Difference Vegetation Index (NDVI) image (Figure 3). The NDVI image will be used to create the Evapotranspiration surface going forward.

Using the NDVI image the vegetation pixel with the highest NDVI value, 0.964577, was located (Figure 4). Then the soil pixel with the lowest NDVI value, .06036, in the study area was located (Figure 5). The minimum and maximum NDVI values were paired with the minimum and maximum Evapotranspiration (ET) values provided by Eve Halper. The maximum or potential ET value was based on the daily temperatures at one of the fluxtower sites in the area. In order to normalize the base NDVI to zero, the soil NDVI value was set to zero and the original soil NDVI value, 0.06036, was subtracted from the vegetation NDVI value, 0.964577. A linear regression was performed using the two normalized points in order to create an equation, $y = 10.396x$, to convert NDVI to ET (Figure 6). Using ERDAS IMAGINE the NDVI values were fed into the regression equation to create a 1 meter ET raster in milimeters per day (Figure 7).

DISCUSSION OF LIDAR DATA

A 1.5 meter raster of bare earth and a 1.5 meter raster of first return from a Light Detection and Ranging (LiDAR) acquistion were examined. The bare earth layer was then subtracted from the first return data to create a 1.5 meter object height model (OHM). The OHM was then resampled to 1 meter to match up with the 1 meter NAIP data. A shift of the OHM was then performed in order to make sure the pixels of the NAIP and OHM overlapped properly. Once the pixels overlapped it was s that there was a bit of misregistration between the two data sets. It was also revealed that a registration of the data may not solve all the problems with the OHM. The LiDAR data seems to have missed a lot of small shrubs along with some larger shrubs (Figure 8). Going forward the plan is to focus in on the areas of main concern, lands containing wells, and attempt to register the LiDAR data to create land cover classifications of irrigated trees, shrubs, and grass.

DISCUSSION OF 15CM AERIAL DATA (SEPTEMBER 2009)

It was discovered that a 4-band (Red, Green, Blue, and Near-Infrared) 15 centimeter aerial was acquired at the same time as the LiDAR data (September 2009). There is somewhat of a disconnect between the aerial imagery and the LiDAR data due to the different spatial resolutions, but the registration is better than the LiDAR and NAIP data. However, the issue of missing objects in the LiDAR is still apparent and will not help to create a more accurate land cover classification of the study region. Another issue with the aerial imagery is time of capture (late September). There is a lot of grass cover at this time of the year making it difficult to discriminate between woody cover and grass without accurate height data (Figure 9). Comparison of the 1 meter NAIP data and the 15 centimeter aerial data showed that the same number of shrubs and trees could be identified in both sets of imagery. However, the 15 centimeter data provided more detail of the smaller shrubs within the study region. It was determined that since the same amount of woody cover could be identified on the NAIP data and since the NAIP data was acquired at a more appropriate time of year, June, the classification was performed with the 1 meter data. Also the 15cm aerial image data were 268GB compared to the NAIP data which were 21GB.

VEGETATION CLASSIFICATION

A classification was performed using the 1 meter NAIP data along with the NDVI created from the NAIP and a Principal Components Analysis (PCA) image. Sample polygons were created in ArcGIS in order to provide training data to the SEE5 Classification and Regression Tree (CART) algorithm. Polygons were created for the following five classes: Trees, Shrubs, Grass, Structures, and Bare Ground. The classification was performed using the SEE5 and ERDAS Imagine software packages. After the classification process the raster product was reclassed in order to combine the Tree and Shrubs classes together and the Structures and Bare Ground classes together. This reclass of the data was performed because the LiDAR data was not included in the classification process. The three class, Tree/Shrubs, Grass, Other, raster achieved an overall accuracy of 99% with a kappa value of 0.98 (Table 1).

Other classifications were attempted with LiDAR along with the multispectral data, but the algorithm became confused. The sparseness of the LiDAR measurements lead to misclasifications in the mountanious regions with a large amount of tree cover and in areas with small shrubs.

In order to integrate the LiDAR data into the classification the following steps were taken. The classification was converted to a binary where the two class were vegetation and not vegetation so the Tree/Shrubs class was integrated with the Grass class (Figure 10). The CHM created earlier was also converted to binary format containing pixels with LiDAR height data and pixels with no height data. The binary land cover classificationa and the binary CHM were combined to create a raster with three classes: vegetation with height, vegetation with no height, and an other class. This process was performed because a more accurate classification of vegetation could be performed without the sparse LiDAR data. Integrating the LiDAR data after the classification process allowed for identification of all the vegetation in the study area and provided information on heights of vegetation where it was available.

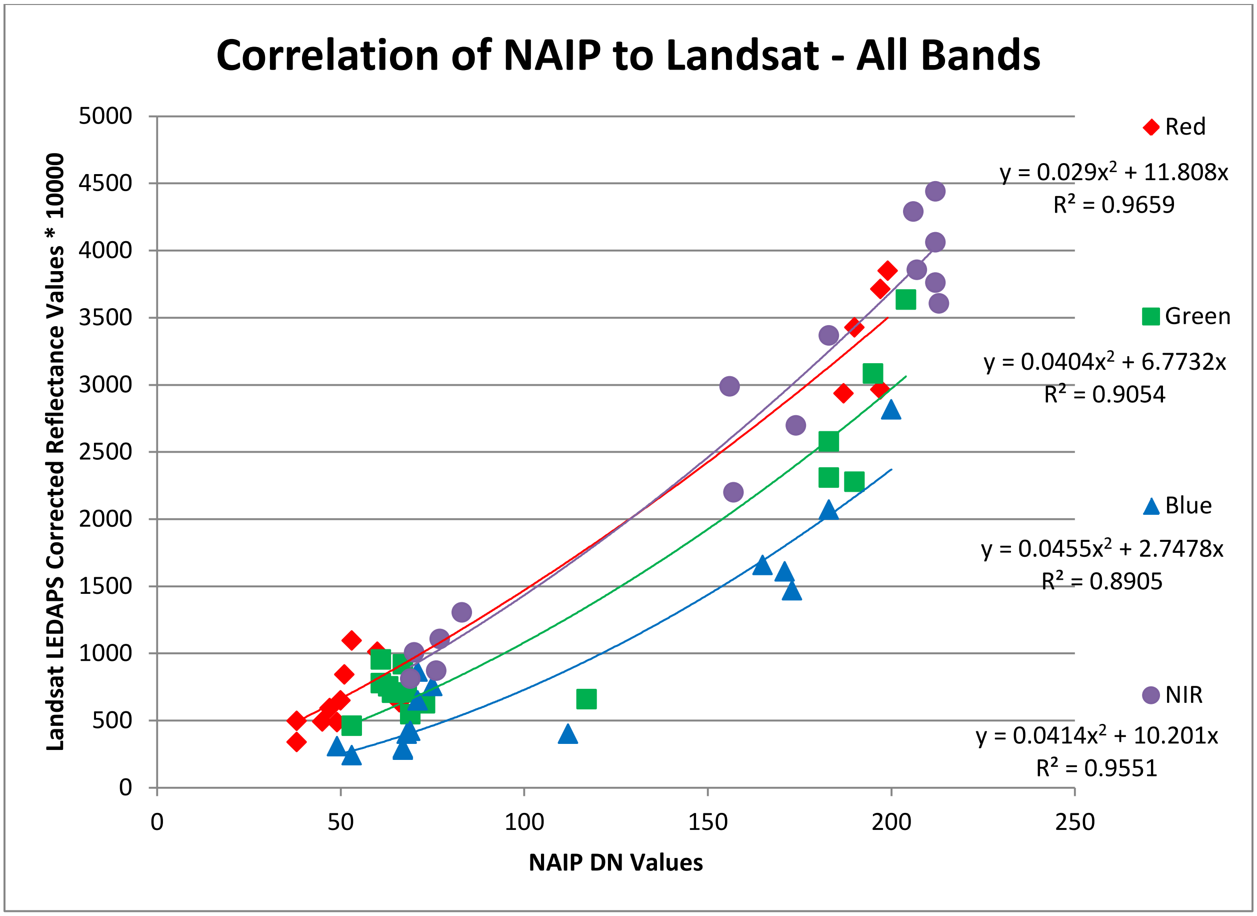

Figure 1: Scatterplot comparing the NAIP DN values (x-axis) to the Landsat LEDAPS Corrected Reflectance Values * 10000 (y-axis) for the Red, Green, Blue, and NIR bands. Each of the bands had a correlation value above .89 and the polynomial fit equations were used to calibrate the NAIP data.

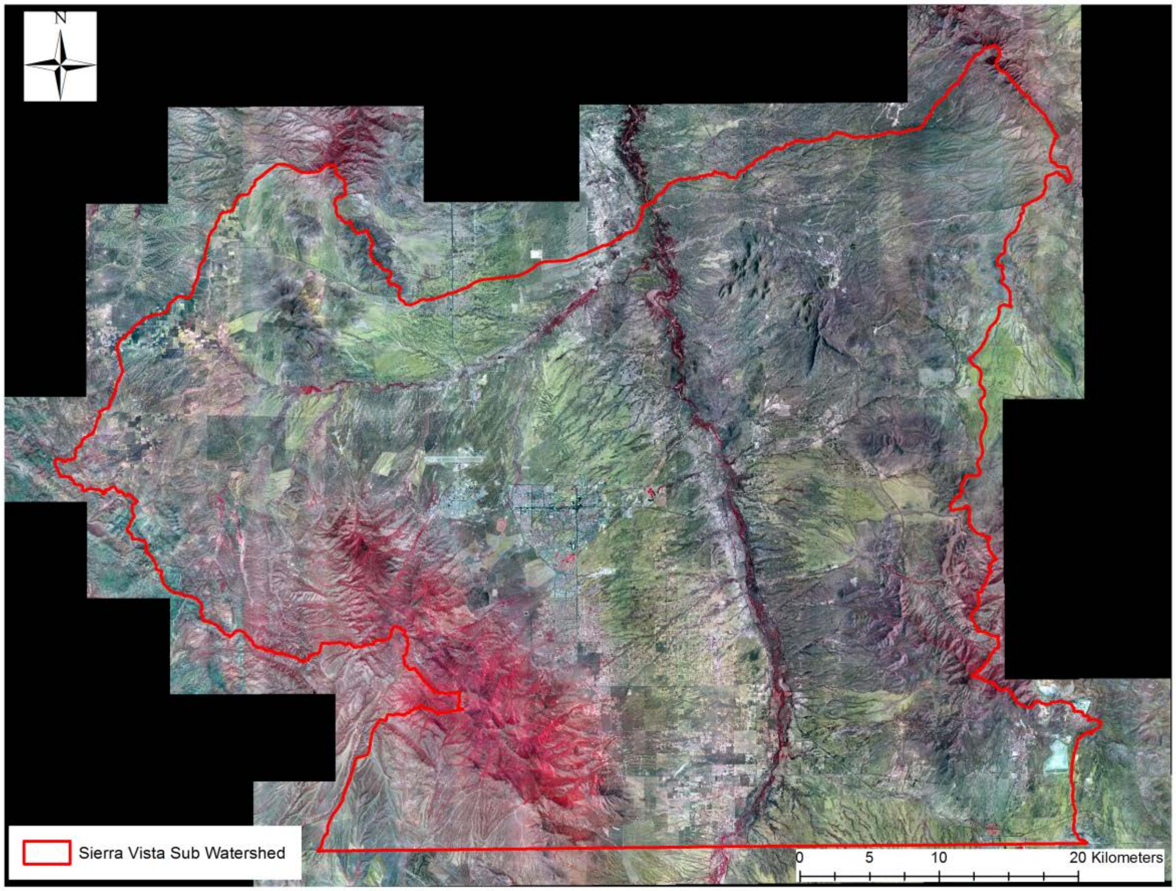

Figure 2: False color composite of Landsat calibrate NAIP mosaic for the study with the Sierra Vista Sub Watershed outlined in red.

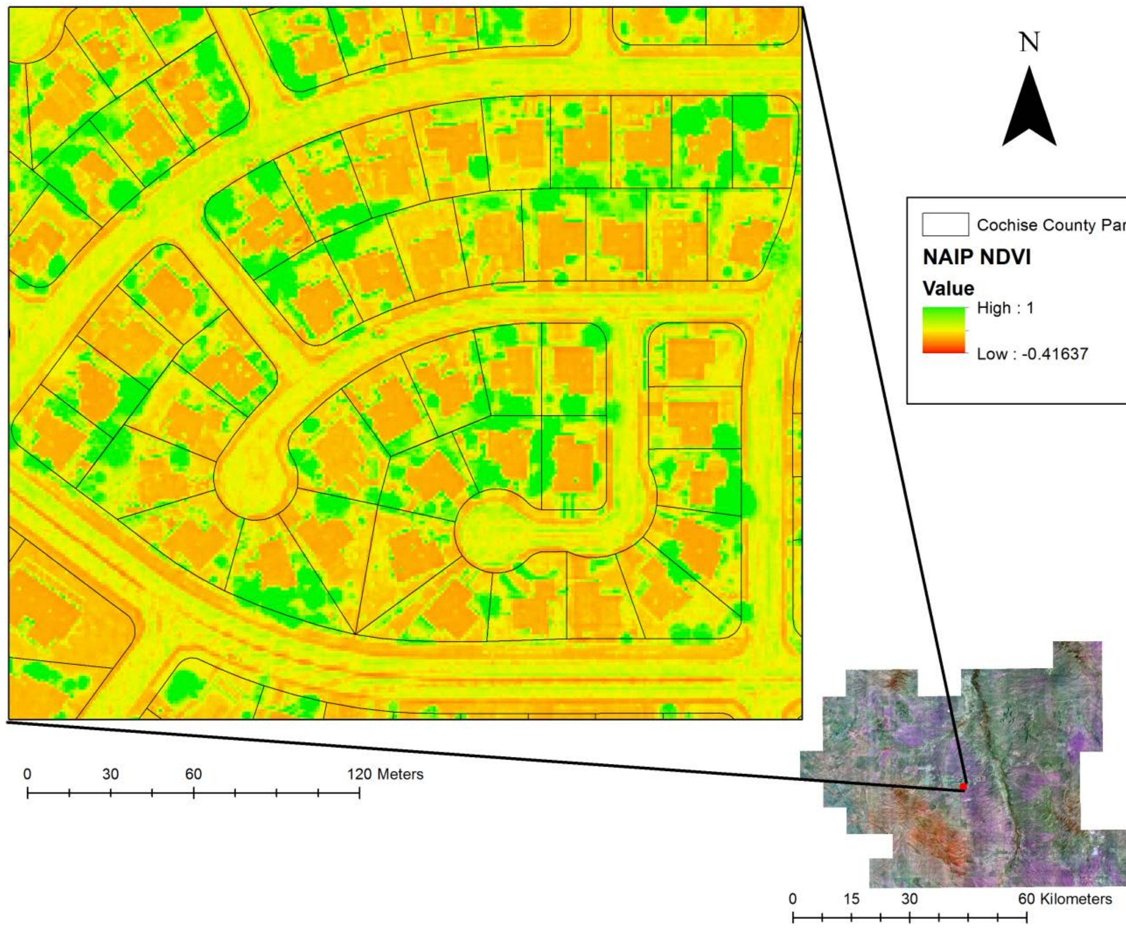

Figure 3: Zoom in on the NDVI layer of a set of residential parcels. The green represents pixels with high NDVI values, while the oranges and yellows represent areas with low NDVI values. The pullout shows where the parcels are located in the overall study area.

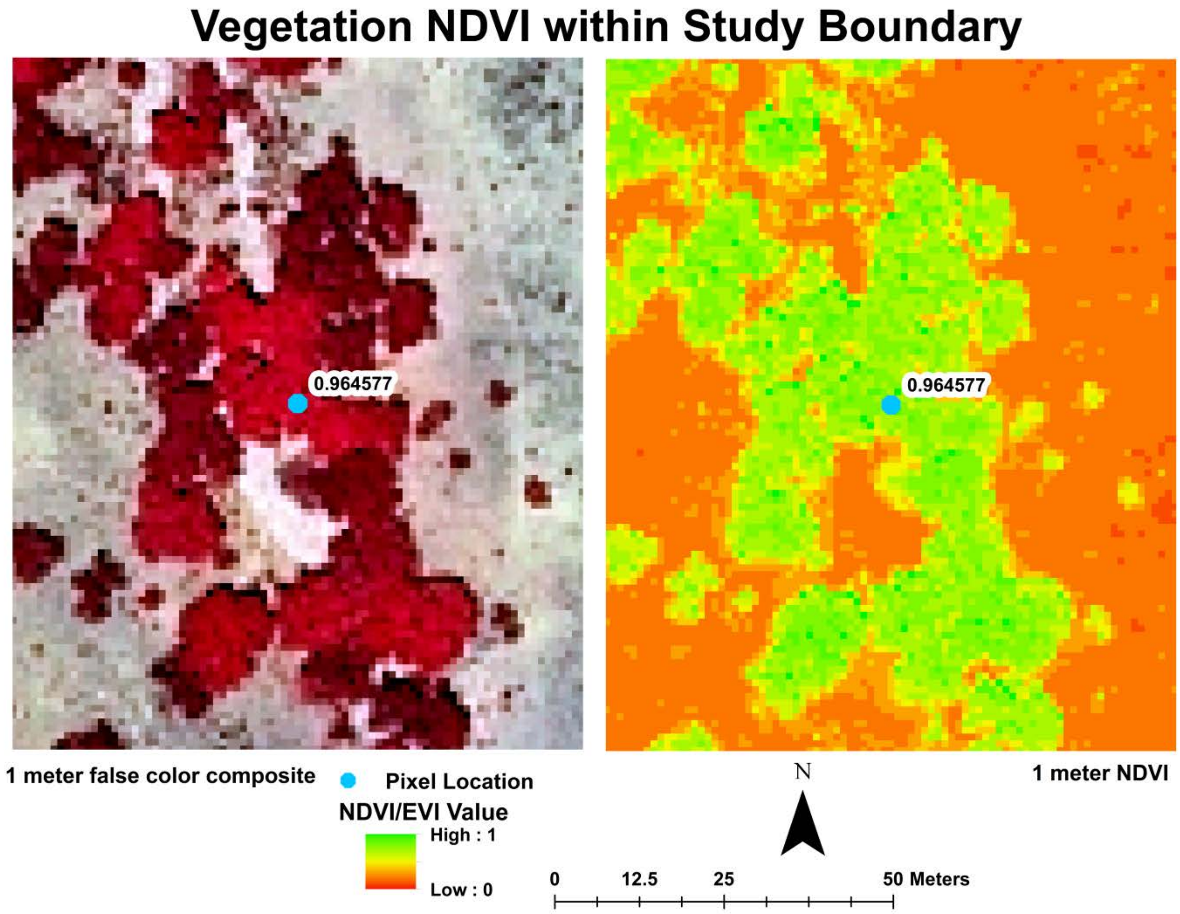

Figure 4: Location of pixel used as maximum NDVI value for Evapotranspiration and NDVI regression.

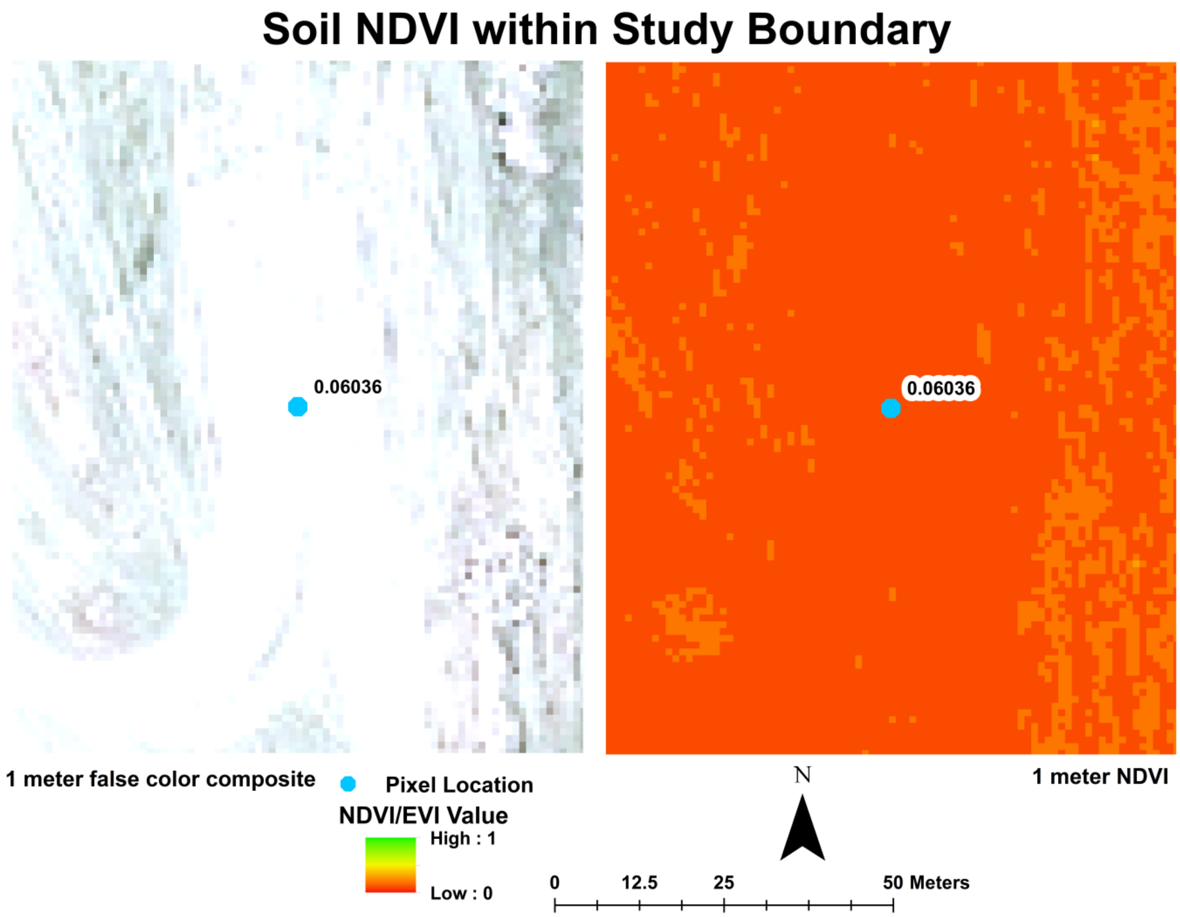

Figure 5: Location of pixel used as minimum NDVI value for Evapotranspiration and NDVI regression.

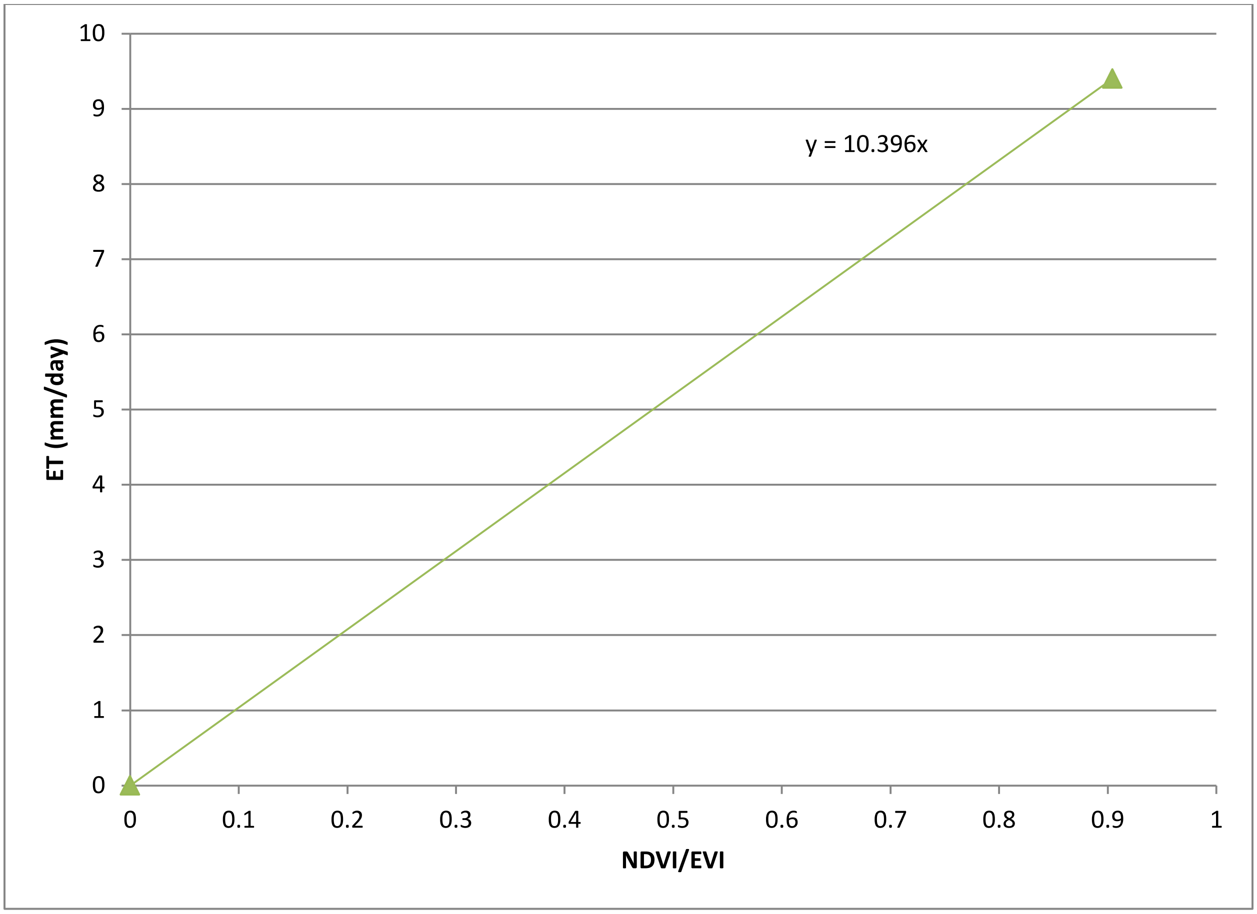

Figure 6: Regression of NDVI and ET data to create equation to convert NDVI data to ET data.

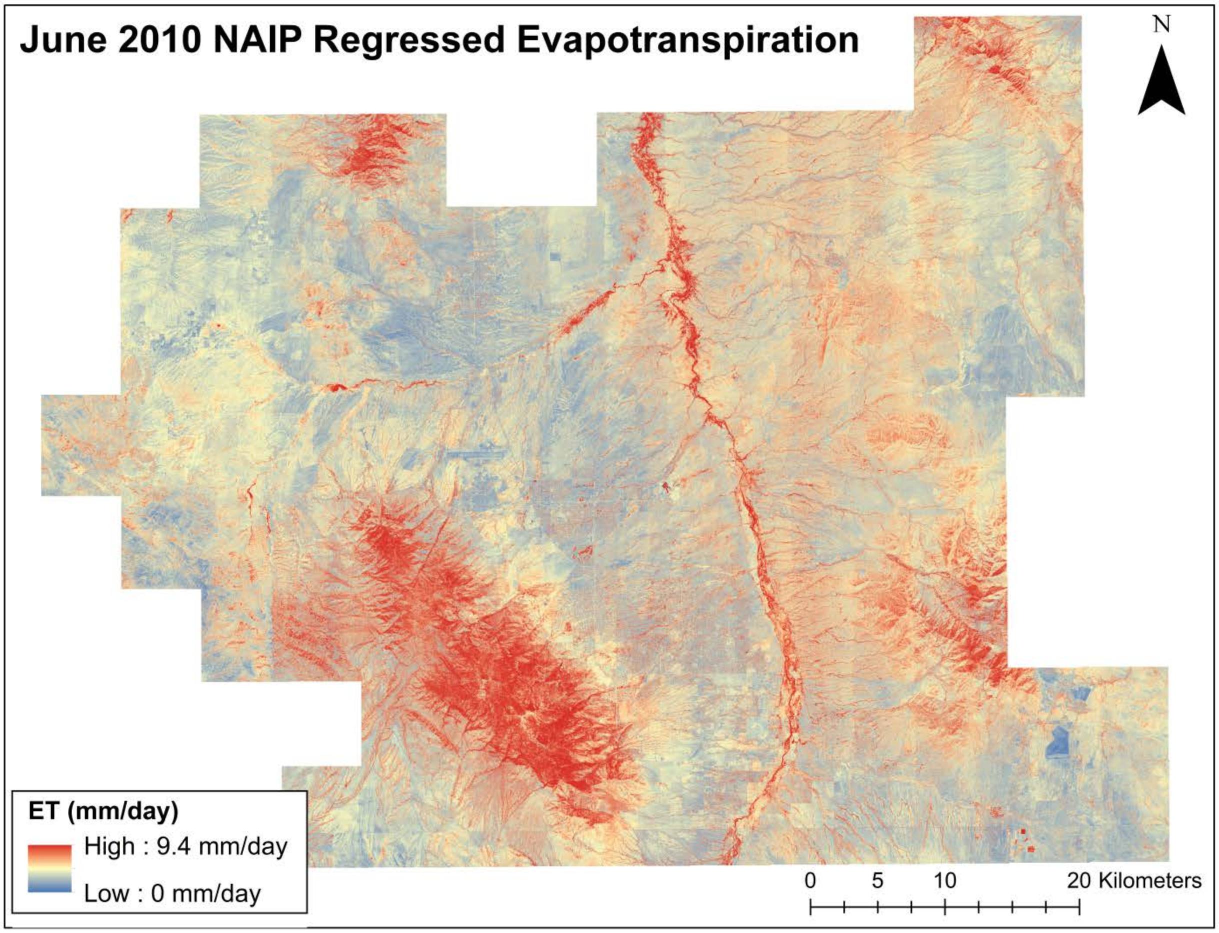

Figure 7: 1 meter ET product created using a linear regression of NDVI and ET data. Higher values of ET are displayed in red, while low values of ET are displayed in blue.

Figure 8: Pixels with height above the ground are displayed in orange. This image shows areas of misregistration along with shrubs that were not captured by the LiDAR data at all (small orange circle at bottom left hand corner).

Figure 9: Subset of 15 centimeter aerial image data captured in tandem with LiDAR data in September of 2009. The image data is displayed in false color showing that it is difficult to discern between trees and grass.

Table 1: Accuracy assessment of classification performed using 1 meter NAIP, NDVI, and PCA image data.

		1	**2**	**3**	**Total**	**User**	**Commission**	**Kappa**
Trees/Shrubs	**1**	**99**	1	0	100	99.0%	1.0%	0.98
Grass	**2**	1	**49**	0	50	98.0%	2.0%	0.97
Other	**3**	0	0	**50**	50	100.0%	0.0%	1.00
	Total	100	50	50	**200**			
	Producer	99.0%	98.0%	100.0%		**198**		
	Omission	1.0%	2.0%	0%			**99.0%**	
	Kappa	0.98	0.97	1.00				**0.98**

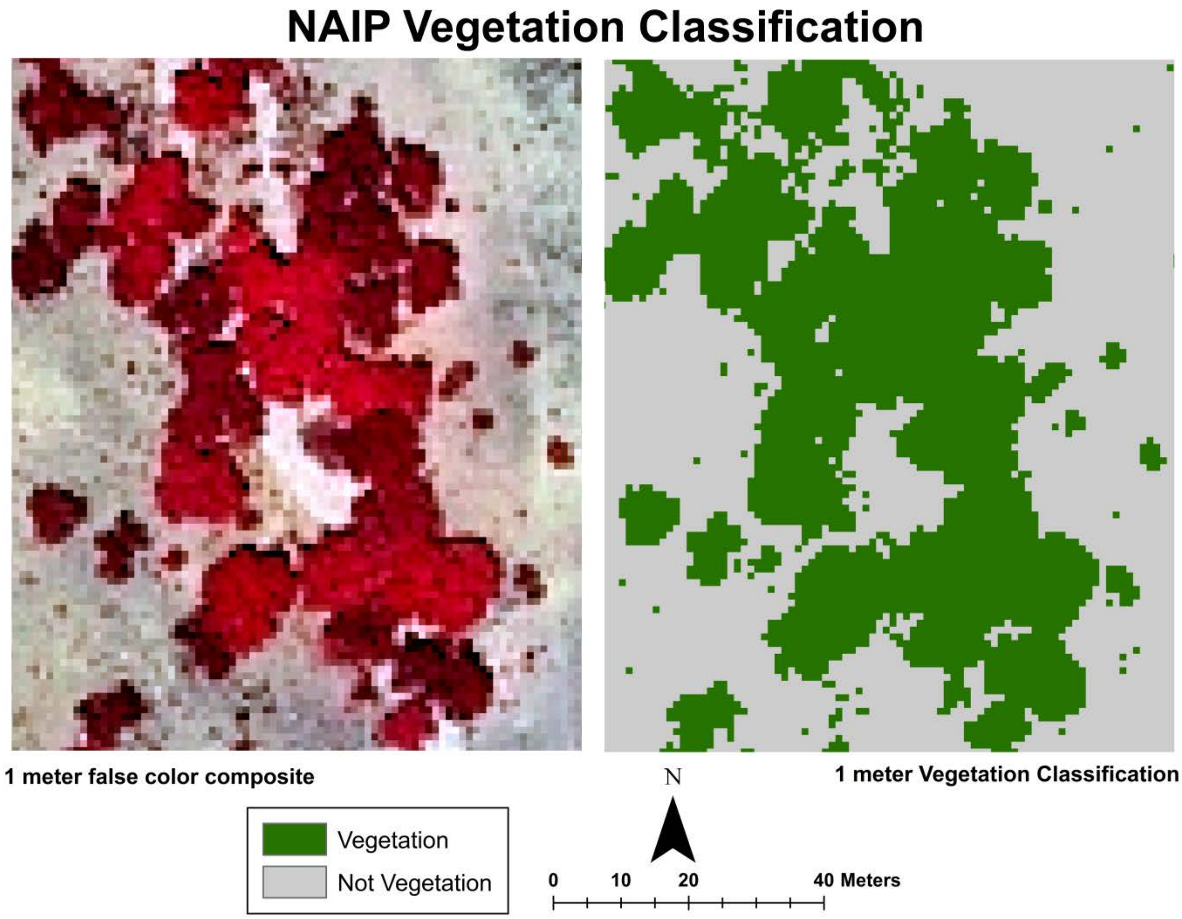

Figure 10: Zoom in on an area showing how the binary vegetation/not vegetation classification created using NAIP, NDVI, and PCA data looks like. The classification is displayed next to the 1 meter NAIP data to show how accurately vegetation was classified.

NAIP Vegetation Classification

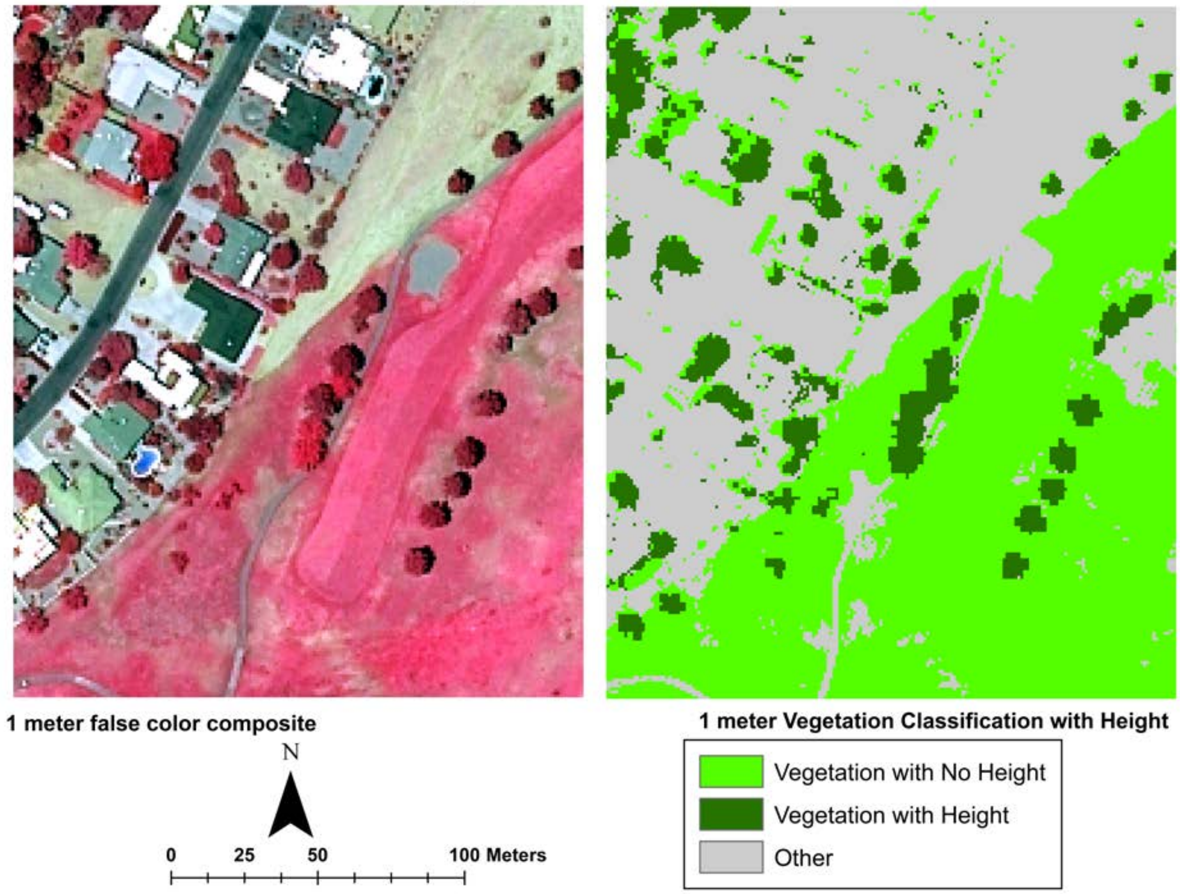

Figure 11: A combination of NAIP Vegetation and LiDAR data was used to create a classification detailing vegetation with and without height which is displayed on the right hand side. The 1 meter NAIP is displayed on the left hand side in false color for comparison purposes.

Final Report:

Integration of High-Resolution Imagery with Meteorologic Data to Estimate Evapotranspiration

Interagency Acquisition R12PG32015

1. Introduction

1.1. Background:

The lack of information on domestic well pumping introduces substantial uncertainty into the regional water balances that form the basis of Reclamation supply augmentation studies. To address this issue, Reclamation's Science and Technology Grant Program funded the proposal, "Estimating Unmetered Ground Water Irrigation Demand with High-Resolution Remote Sensing Data". The initial steps of the project, to be performed by the University of Arizona Remote Sensing Center, will integrate a Geographic Information System (GIS) and high-resolution remote sensing data to identify vegetation irrigated with domestic wells. USGS staff will then combine the spatial data products with meteorological observations to estimate evapotranspiration (ET) by irrigation-supported vegetation. The area of interest is the Sierra Vista Subwatershed (SVS) in southeastern Arizona, site of an ongoing Reclamation feasibility study.

1.2. Objectives:

The work described in this agreement is a critical step in the development of a method to estimate the water use of irrigated vegetation for unmetered wells. The technique uses GIS data and high-resolution remote sensing data, which are increasingly available in many communities, to identify vegetation irrigated with domestic wells and integrates it with widely available meteorological data to estimate evapotranspiration rates. Our area of focus is the SVS in southeastern Arizona, but methods should be generalizable to other areas, especially to arid and semi-arid regions.

2. Investigation Outline

2.1. *Phase 1: Estimate Residential Irrigation Demand from Domestic Wells/ Water Providers in SVS using Enhanced Vegetation Index (EVI) and meteorological variables*

2.1.1. Part A.

Using previous research relating in-situ measurements and meteorological data, develop site specific relationship between evapotranspiration data and local air temperature maxima for the SVS area.

2.1.2. Part B.

Extrapolate maximum air temperature surface across SVS.

2.1.3. Part C.

Generate map of evapotranspiration for vegetation indices derived for high National Agriculture Imagery Program (NAIP) or Quickbird (a high-resolution commercial earth observation satellite) and low resolution Moderate Resolution Imaging Spectroradiometer (MODIS) remotely sensed data.

2.2. *Phase 2: Estimate Residential Irrigation Demand from Domestic Wells/ Water Providers in area of Fort Huachuca Orthophotography/ Light Detection and Ranging (LIDAR) acquisition using plant-type coefficients.*

2.2.1. Part A.
Derive vegetation canopy surface for subset of SVS from combination of four-band orthophotography and LIDAR data. Subtract from bare earth digital elevation model (DEM) to derive canopy height model. Refer to dry season 2007 NAIP orthophotography to distinguish between irrigated and non-irrigated areas on residential properties, as in Phase 1. Use previously derived GIS cover to identify residential properties dependent on domestic wells.

2.2.2. Part B.
Use texture measures and LIDAR canopy height to categorize irrigated residential vegetation into trees, grass and shrubs. Assign USGS/Reclamation supplied plant-type coefficients and multiply by Eto to derive maps of irrigated vegetation ET demand.

3. List of Deliverables:

1. Develop site-specific relationship between evapotranspiration data and local air temperature maxima for the SVS area.

2. Generate map of evapotranspiration for vegetation indices derived for high (NAIP or Quickbird) and low resolution (MODIS) remotely sensed data.

3. Derive vegetation canopy surface for subset of SVS from combination of four-band orthophotography and LIDAR data.

4. Use texture measures and LIDAR canopy height to categorize irrigated residential vegetation into trees, grass and shrubs.

Except for deliverable 1, deliverables were transmitted in the form of GIS files, conveyed on a portable hard drive acquired specifically for the project. Deliverables 2, 3, and 4 are visualized in the Figures A, B and C below.

Deliverable 1:

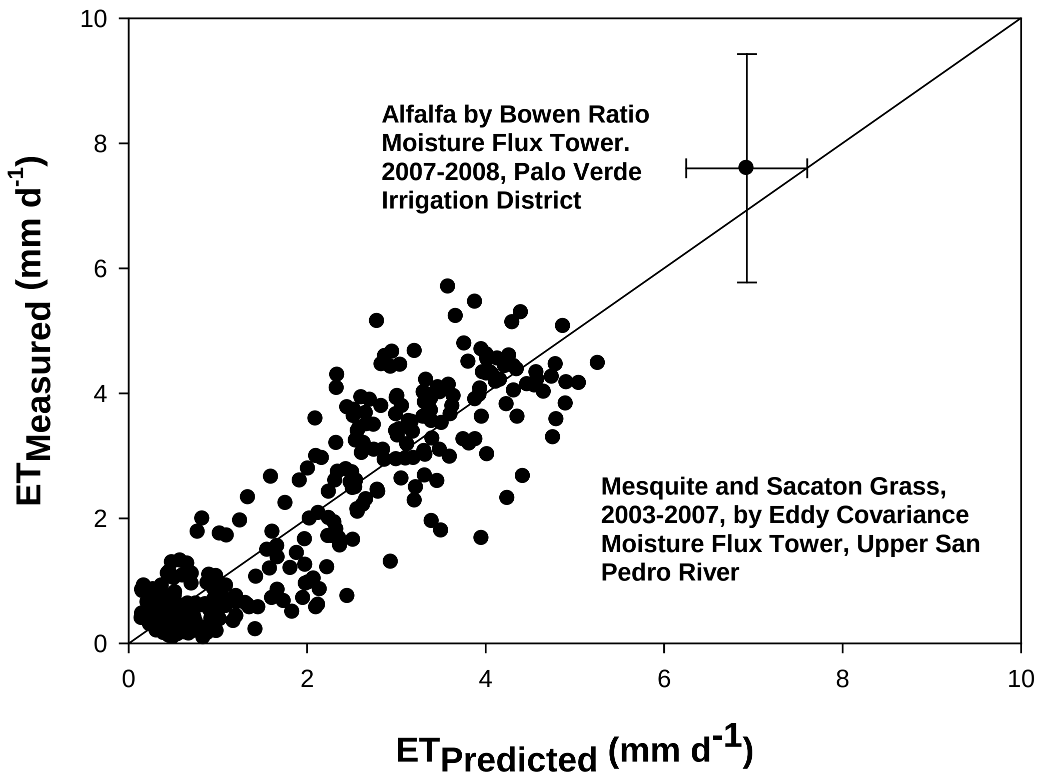

Predictive Equation:

$ET = 1.098ET_o(1-e^{-1.67NDVI^*}) + 0.146$, $r^2 = 0.81$
$NDVI^* = 1 - (NDVI_{Max} - NDVI)/(NDVI_{Max} - NDVI_{Soil})$
$NDVI_{Max} = 0.880$ (from Kansas Settlement Center Pivot fields)
$NDVI_{Soil} = 0.171$ (from winter San Pedro tower sites)
Equation was developed from San Pedro Data and co-plotted with alfalfa data for comparison

ETo (from Kansas Settlement AZMET):

mm/day

Jan	1.85	Jul	6.64
Feb	2.13	Aug	5.57
Mar	4.26	Sept	4.75
Apr	5.08	Oct	3.69
May	7.13	Nov	2.79
June	8.03	Dec	2.30

Total Annual (mm/year): 1686

Figure A: Map of evapotranspiration for vegetation indices derived for high (NAIP or Quickbird) and low resolution (MODIS) remotely sensed data (Deliverable 2)

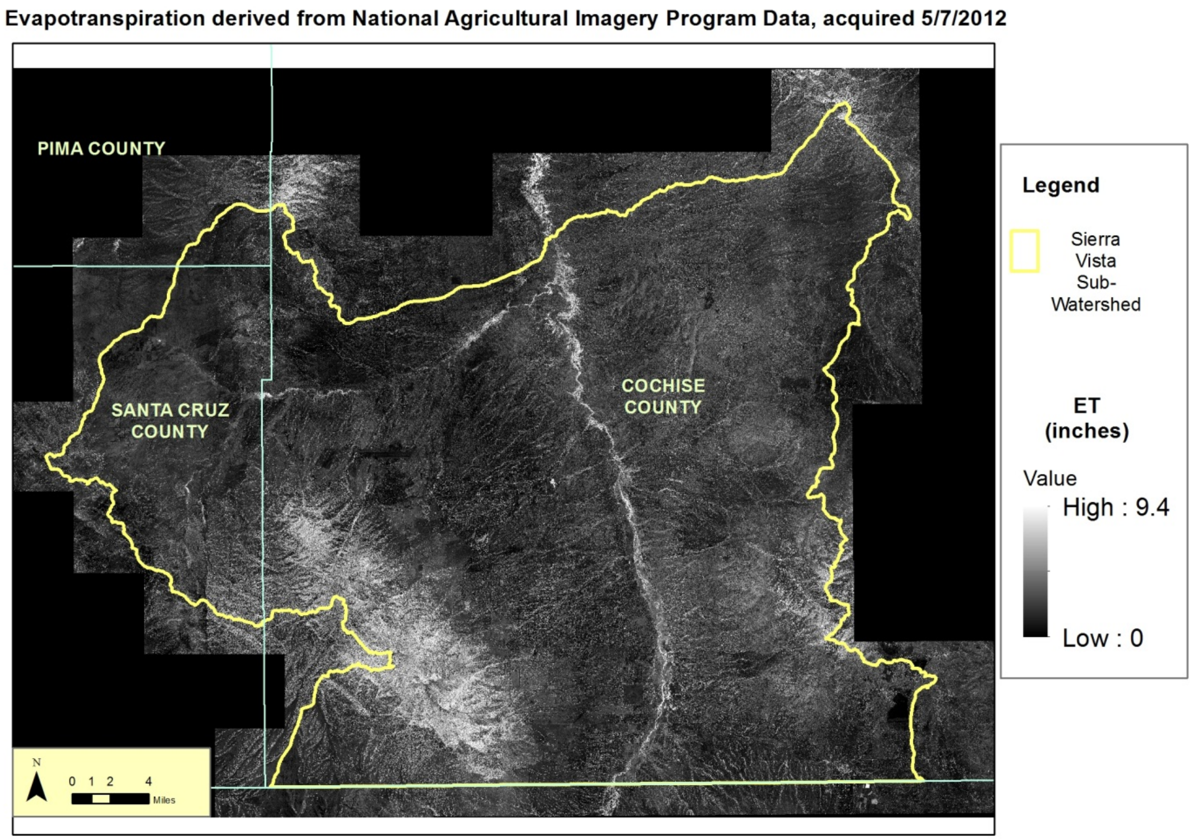

Figure B: Map of vegetation canopy surface for subset of SVS (Deliverable 3)

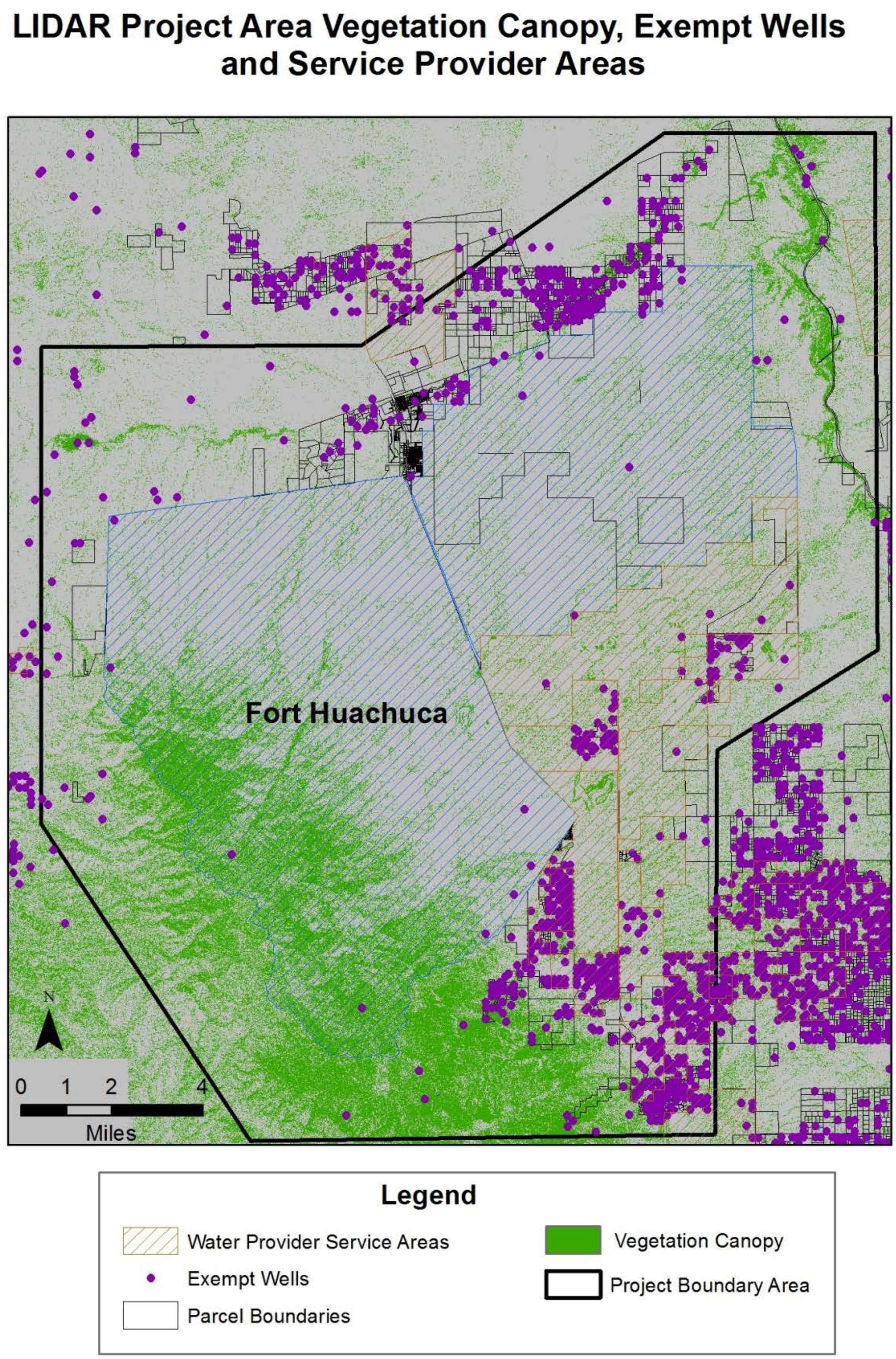

Figure C: Map of evapotranspiration using four-band orthophotography and LIDAR data to distinguish between vegetation types (Deliverable 4)

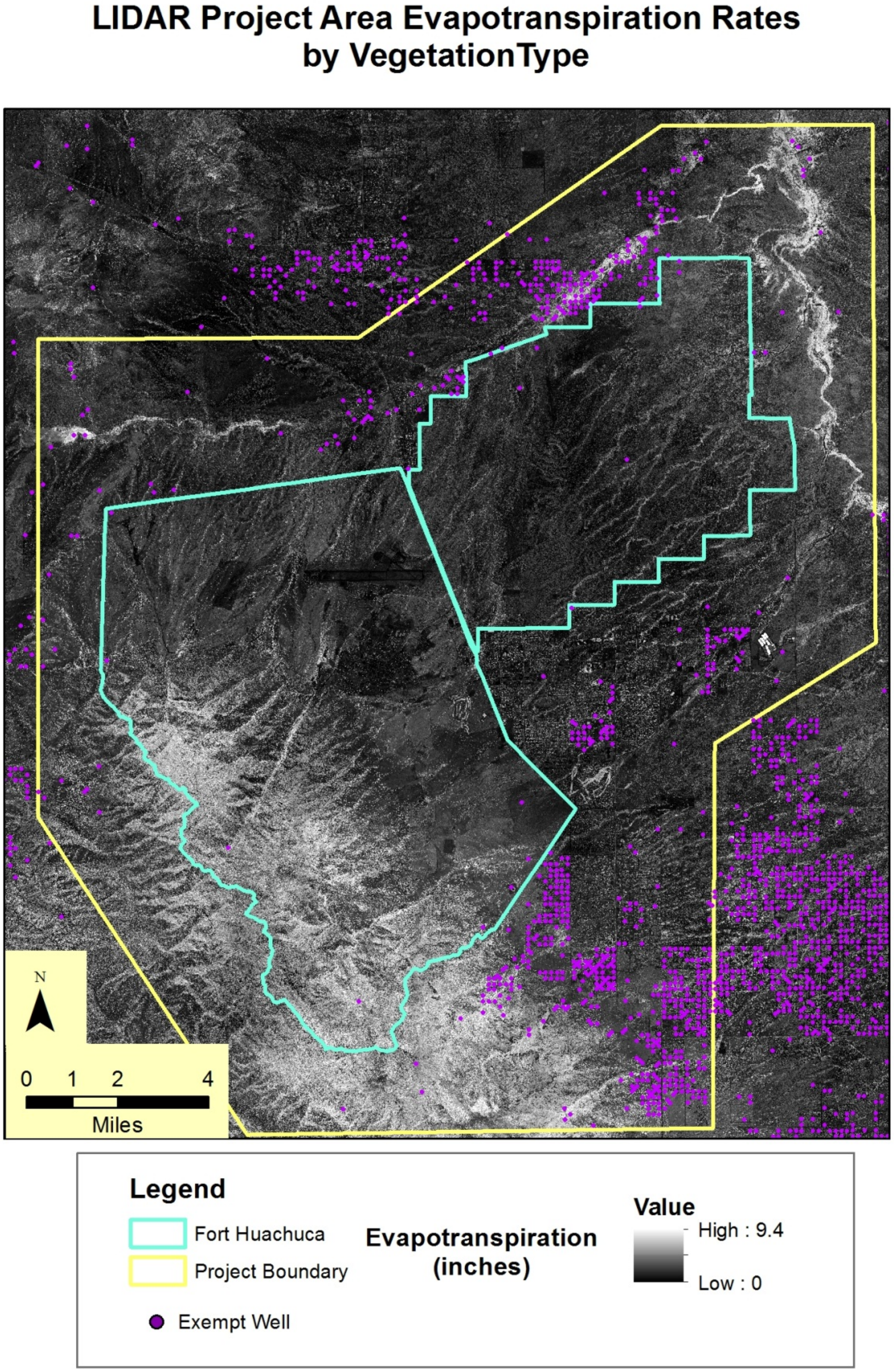

4. References and Notes

1. Glenn, E.; Morino, K.; Didan, K.; Jordan, F.; Nagler, P.; Waugh, J.; Carroll, K.; Sheader, L. Scaling sap flux measurements of grazed and ungrazed shrub communities with fine and coarse-resolution remote sensing. *Ecohydrol.* **2008**, *1*, 316-329.

2. Gonzalez-Dugo, M.P.; Neale, C.M.U.; Mateos, L.; Kustas, W.P.; Anderson, M.C.; Li, F. A comparison of operational remote-sensing based models for estimating crop evapotranspiration. Agr. Forest Meteor. **2009**, 49, 2082-2097.

3. Groeneveld, D.P.; Baugh, W.M.; Sanderson, J.S.; Cooper, D.J. Annual groundwater evapotranspiration mapped from single satellite scenes. J. Hydrol. **2007**, 344, 146-156.

4. Hunsaker, D.J.; Fitzgerald, G.J.; French, A.N.; Clarke, T.R.; Ottman, M.J.; Pinter, P.J. Wheat irrigation management using multispectral crop coefficients. I. Crop evapotranspiration prediction. Trans. ASABE **2007**, 50, 2017-2033.

5. Juarez, R.I.N.; Goulden, M.L.; Myneni, R.B.; Fu, R.; Bernardes, S.; Gao, H. An empirical approach to retrieving monthly evapotranspiration over Amazonia. Int. J. Remote Sens. 2008, 29, 7045-7063.

6. Kim, J.Y.; Hogue, T.S. Evaluation of a MODIS-based potential evapotranspiration product at the point scale. J. Hydrometeor. **2008** 9, 444-460.

7. Leuning, R.; Zhang, Y.Q.; Rajaud, A.; Cleugh, H.; Tu, K. A simple surface conductance model to estimate regional evapotranspiration using MODIS leaf area index and the Penman-Monteith equation. Water Resour. Res. 2008, 44, Article No. W10419.

8. Nagler, P.L.; Glenn, E.P.; Kim, H.; Emmerich, W.; Scott, R.L.; Huxmam, T.E.; Huete, A.R. Relationship between evapotranspiration and precipitation pulses in a semiarid rangeland estimated by moisture flux towers and MODIS vegetation indices. *J. Arid. Environ.* **2007**, *70*, 443-462.

9. Nagler, P.; Scott, R.; Westenburg, C.; Cleverly, J.; Glenn, E.; Huete, A. Evapotranspiration on western US rivers estimated using the Enhanced Vegetation Index from MODIS and data from eddy covariance and Bowen ratio flux towers. *Remote Sens. Environ.* **2005**, *97*, 337-351.

10. Nagler, P.L.; Morino, K.; Didan, K.; Osterberg, J.; Hultine, K.; Glenn, E. Wide-area estimates of saltcedar (Tamarix spp.) evapotranspiration on the lower Colorado River measured by heat balance and remote sensing methods. *Ecohydrol.* **2009**, *2*, 18-33.

11. Zhang, Y.Q.; Chiew, F.H.S.; Zhang, L.; Leuning, R.; Cleugh, H.A. Estimating catchment evaporation and runoff using MODIS leaf area index and the Penman-Monteith equation. *Water Resou. Res.* **2008**, *44*, Article No. W10420.